Deep–Sea Research II 202 (2022) 105151

Contents lists available at ScienceDirect

Deep-Sea Research Part II

journal homepage: www.elsevier.com/locate/dsr2

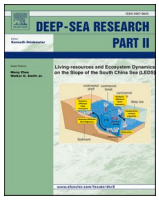

Retention properties of the Agulhas bank and their relevance to the *chokka* squid life cycle

Zoe Jacobs [a,*], Stephen Kelly [a], Fatma Jebri [a], Michael Roberts [a,b], Meric Srokosz [a], Warwick Sauer [c], Lisa Hancke [b], Ekaterina Popova [a]

[a] National Oceanography Centre, Southampton, SO14 3ZH, United Kingdom
[b] Nelson Mandela University, Gqeberha, 6001, South Africa
[c] Department of Ichthyology and Fisheries Science, Rhodes University, Makhanda, South Africa

A B S T R A C T

Retention is thought to be a crucial component required to create a favourable habitat for coastal pelagic species. It is vital for the survival of 'chokka' squid (*Loligo reynaudii*), which is a fishery that supports thousands of people living in the Eastern Cape of South Africa. After chokka spawn, retention on the Agulhas Bank is crucial to prevent starvation in the early life stages. Using a high-resolution ocean model, this study quantifies retention properties of the Agulhas Bank most relevant to the chokka squid. We estimate the proportion of virtual Lagrangian particles, representing paralarvae, that are retained on the Agulhas Bank within 30 days after being released from the main chokka squid spawning sites. Over an 18-year period (1995–2013), considerable variability is found on seasonal and interannual timescales, with the greatest retention occurring for particles released further to the west. The greater losses for the easternmost release sites are due to increased interaction with the Agulhas Current. While 90–100% retention is the most common scenario, high loss (>50%) events are also apparent and are associated with different variability modes of the Agulhas Current. These variability modes include i) meanders that cause offshore flow at the northeast edge of the Bank, ii) the presence of a fast, onshore branch of the Agulhas Current rapidly advecting the particles off the Bank further west (associated with a Natal Pulse) and iii) an Agulhas Current positioned further south of the Bank leading to an offshore flow from the eastern Agulhas Bank. The third variability mode usually occurs 1–2 months after the passage of a Natal Pulse or meander. However, 1–2 weeks after the passage of a Natal Pulse, retention increases, so the timing of these events relative to particle release is crucial. This shows that the key to understanding paralarvae retention lies both in the occurrence of these dynamic features and in their timing relative to the spawning events.

1. Introduction

The 'chokka' squid *Loligo Reynaudii* fishery is vital to sustain the livelihoods of ~25,000 people living in the Eastern Cape of South Africa (Cochrane et al., 2014). With a highly variable catch, it is important to understand what drives fluctuations in chokka biomass, which is largely related to changes in the ecosystem on the Agulhas Bank (AB; e.g., Roberts, 2005). The lifespan of chokka squid is only one to two years (Sauer et al., 1997). They spawn during the austral summer from November to April (Cochrane et al., 2014) in waters shallower than ~60 m between Plettenberg Bay and Port Alfred, Fig. 1 (e.g., Augustyn et al., 1994; Lipiński et al., 2016). Bottom temperatures from 12 to 17 °C and dissolved oxygen concentrations of >3 ml l^{-1} favour embryonic development, making this region optimal for spawning (Roberts, 2005). Once they have spawned, surface currents transport some of the paralarvae towards the central AB, which offers rich feeding grounds (Roberts, 2005; Hutchings et al., 2009). In addition to wind-driven and current-driven upwelling at the eastern coast (Leber et al., 2017), this region is also the site of a seasonal productive feature known as the 'Cold Ridge' (Swart and Largier, 1987; Jacobs et al., *this issue*). The high density of copepods that has been recorded in the vicinity of the Cold Ridge (Huggett and Richardson, 2000) makes it an ideal feeding ground for the chokka paralarvae (Roberts, 2005). Both juvenile and adult chokka make use of the wider AB and the Benguela upwelling area (west coast of South Africa) to feed before returning east to spawn (Augustyn et al., 1992). However, low retention of paralarvae on the AB can occur, which will cause starvation and greatly impact recruitment strength and potential catches (e.g., Roberts, 2005).

The few 100 km separating the spawning area from the feeding grounds suggests that currents are likely to play an important role in the chokka squid life cycle (Roberts, 2005). Prevailing surface currents are westward during peak spawning (Roberts and Van den Berg, 2002) but there is evidence for mixed flow patterns on the AB, especially further inshore (Roberts and Van den Berg, 2002; Roberts and Mullon, 2010).

* Corresponding author.
E-mail address: zoe.jacobs@noc.ac.uk (Z. Jacobs).

https://doi.org/10.1016/j.dsr2.2022.105151
Received 18 November 2021; Received in revised form 20 June 2022; Accepted 3 July 2022
Available online 12 July 2022

The broad westward flow on the mid-shelf is exploited by the chokka paralarvae to optimise these two separate environments (i.e., spawning on the eastern AB and feeding on the central AB) and is known as the 'westward transport hypothesis' (Roberts, 2005). Prior regional modelling (ROMS) studies have found that the most successful spawning sites, i.e., where paralarvae reach the central AB, occur from spring to autumn, when currents are strongest, and when released further west (see Fig. 1; Martins et al., 2014; Downey-Breedt et al., 2016). The spawning sites west of St Francis are less likely to encounter the fast flow of the Agulhas Current (AC). In contrast, the spawning sites located further east are more likely to encounter the AC, which may lead to large offshore losses (e.g., Roberts and Van den Berg, 2002; Roberts and Mullon, 2010).

The AC is one of the strongest western boundary currents in the world and flows south-westwards along the east coast of South Africa (e.g., Lutjeharms, 2006), considerably influencing the dynamics on the AB. It is most intense north of ~34°S, reaching speeds of up to 2.6 m s^{-1}, where it flows close to the narrow continental shelf and is fairly stable (Lutjeharms, 2006). Further south, the AC diverges from the coast and becomes more unstable where the shelf widens to form the AB (Lutjeharms et al., 1989). The AC interacts more strongly with the Bank further east upstream of Port Elizabeth (now Gqeberha) (~26°E, Boyd et al., 1992) where it was found to be within 20 km of the 200 m isobath 90% of the time, which reduces to only 28% at the southern tip of the Bank (Lutjeharms et al., 1989). There is evidence for offshore flow into the AC near Port Elizabeth (Goschen and Schumann, 1988), with particle losses found to be greater in the austral winter, from May to July (Martins et al., 2014; Downey-Breedt et al., 2016). This coincides with the time period when the AC is weaker compared with a stronger AC in summer (Lutjeharms, 2006; Krug and Tournadre, 2012; Beal et al., 2015; Beal and Elipot 2016; Hutchinson et al., 2018; Lamont et al., 2021). While there are limited observational studies on the seasonal variation in the position of the AC, Lamont et al. (2021) found evidence for a more onshore AC upstream of the AB during the austral summer. Interannual variability in the speed and position of the AC is also recorded at 24°E (Malan et al., 2019).

There is some evidence that changes in the path of the AC can induce offshore flow and reduce retention of paralarvae on the Bank. For example, the abrupt southeastward turn of the AC that occurred during 1999 (later attributed to an early retroflection event (Russo et al., 2021)) led to a considerable loss of biological material from the shelf (observed using satellite remote sensing), which was consequently lost from the AB ecosystem (Roberts and Van den Berg, 2002; Roberts and Mullon, 2010). Additionally, eddies or large solitary meanders known as Natal Pulses (Lutjeharms and Roberts, 1988) can displace the AC by 50–200 km (Gründlingh, 1979; Rouault et al., 2010; Leber and Beal, 2014). These mesoscale features are a major driver of variability at the eastern edge of the Agulhas Bank (Krug et al., 2014) and can increase the risk of offshore losses (Goschen and Schumann, 1988; Lutjeharms et al., 1989; Jackson et al., 2012). As Natal Pulses occur up to 6 times a year (de Ruijter et al., 1999), they could cause considerable offshore losses of chokka paralarvae, leading to recruitment failure and subsequent low catches if they occur during peak spawning periods (Roberts and Mullon, 2010).

As was first suggested by Bakun (1998), there is a 'fundamental triad' of major processes required for favourable habitat for coastal pelagic fish. These are enrichment processes (e.g., upwelling), concentration processes (convergence at frontal zones) and processes leading to retention (Bakun, 1998). The life cycle of chokka squid, like many species, starts with a stage of passive larval drift, and loss at these early life stages affects recruitment (Roberts and Van den Berg, 2002; Vidal et al., 2009), highlighting the importance of retention on the Agulhas Bank. Once the chokka squid have matured enough to be able to control their own movement, they are able to move against the prevailing currents and travel to feeding grounds themselves, which is thought to occur from around 30–45 days (Yang, 1983; Bigelow, 1992; Roberts and Van den Berg, 2002; Vidal et al., 2009). This suggests that, to avoid early starvation, the currents on the Bank are an important mechanism that transport the paralarvae to the main feeding grounds on the central AB, leading to successful recruitment (Roberts, 2005). At the same time, the powerful AC can also exert a major influence on the retention of paralarvae on the Bank.

Following the idea of Bakun's Triad, this study aims to address retention properties of the AB using a high-resolution ocean model. Using a Lagrangian modelling approach, we quantify the proportion of virtual particles, representing paralarvae, that are retained on the Agulhas Bank after being released from the main spawning sites of chokka squid. Building on the work of Roberts and Van den Berg (2002), Roberts and Mullon (2010), Martins et al. (2014) and Downey-Breedt et al. (2016), long-term (1995–2013) variability is investigated on monthly timescales to quantify seasonal and interannual variability of retention properties. Additionally, specific events are analysed in relation to AC dynamics to understand what drives large offshore losses or high retention.

Section 2 describes the model, the Lagrangian tool employed and the experimental setup. The results are presented in section 3, including seasonal and interannual variability of retention, high loss events and high retention events. The discussion and conclusions are provided in sections 4 and 5 respectively.

2. Methods

2.1. Model

The global ocean model Nucleus for European Modelling of the

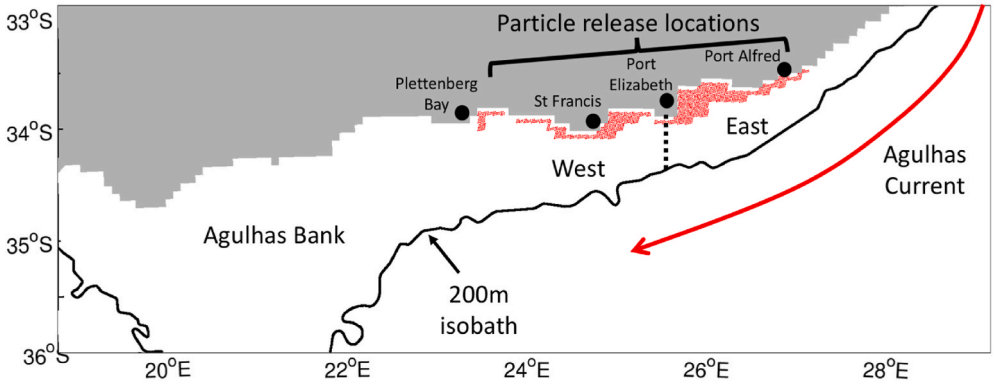

Fig. 1. Schematic of the Agulhas Bank. Shaded red area indicates particle release locations for Lagrangian experiments, the dashed black line at 25.5°E separates East and West releases, the bold black line (the 200 m isobath) defines the edge of the Agulhas Bank and the red line indicates the southwestward flow of the Agulhas Current.

Ocean (NEMO) version 3.6 (Madec, 2015) is utilised in this study. The high, eddy-resolving resolution, 1/12° hindcast ORCA12 is employed (Marzocchi et al., 2015; Moat et al., 2016; Jacobs et al., 2020), which corresponds to approximately 9.25 km at the equator and 7.5 km at 35°S. NEMO is a z-level, hydrostatic model with a nonlinear free surface that has 75 vertical levels, which are more finely spaced near the surface (<1 m at the surface), with 22 levels in the upper 100 m. The model is tri-polar with two North Poles to prevent numerical stability where the meridians converge in the northern hemisphere, with one South Pole (Madec and Imbard, 1996). Sea ice is represented by the Louvain la Nueve sea-ice model (Timmermann et al., 2005). The bottom topography is represented as partial steps with bathymetry derived from ETOPO2 (US Department of Commerce 2006) and a free-slip lateral friction condition applied at the lateral boundaries. Vertical mixing is simulated using the turbulent kinetic eddy scheme (Blanke and Delecluse, 1993) and the total variance dissipation advection scheme is used for active tracers (Cravatte et al., 2007).

The climatological fields from the World Ocean Database (Levitus et al., 1998) are used to initialise the run, which is forced by the Drakkar Surface Forcing dataset version 5.2. This dataset supplies 2 m air temperature, 2 m humidity and 10 m winds, surface radiative fluxes and precipitation, at 0.7° horizonal resolution (Brodeau et al., 2010; Dussin et al., 2016). To avoid excessive drift in global salinity, sea surface salinity is relaxed towards the climatology. The hindcast spans the period 1958–2015 and model output is stored as 5-day means. Here, the period 1995–2013 is analysed. More detailed information on the model can be found in Madec (2015).

2.2. Model validation

Modelled surface currents are compared with gridded altimetry currents over the wider Agulhas Bank region to assess the ability of the model to simulate the circulation (Fig. 2). There is good qualitative agreement between the model and the satellite observations at monthly and decadal timescales, with the model capable of simulating the position and speed of the AC, including the position of the retroflection and the production of Agulhas rings. Additionally, it is able to adequately simulate the mesoscale variability (i.e., eddies and meanders). Some of these features are known problems for global and regional models of varying resolution (e.g., Penven et al., 2010). Furthermore, the model simulates the much weaker currents on the Agulhas Bank with net westward flow over the mid-shelf, consistent with ADCP measurements (Boyd et al., 1992; Boyd and Shillington, 1994). However, the spatial resolution of the model may limit its ability to resolve sub-mesoscale processes that are commonly associated with shelf regions. Here, the spatial (1/12°) and temporal (5-day means) resolution of the model is appropriate to address the aims of the study outlined in section 1, i.e., understanding the seasonal and interannual variability of retention on the Bank and identifying pathways that lead to high or low retention.

2.3. Lagrangian experiments

This hindcast provides input data for the particle-tracking tool, Ariane, an offline mass-preserving Lagrangian scheme (Blanke and Raynaud, 1997), to run Lagrangian experiments investigating retention

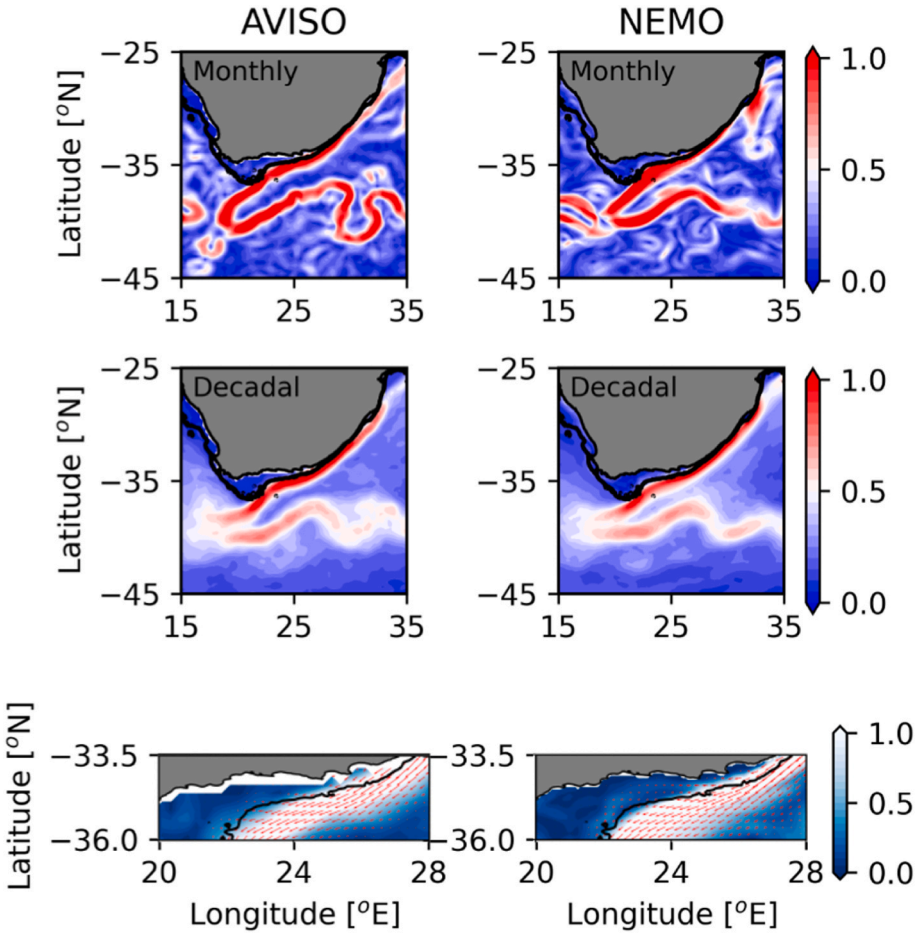

Fig. 2. Surface currents (m s^{-1}) over the South African region in AVISO (left) and in the model (right) showing examples of a monthly mean (top; March 2006) and a decadal mean (middle; averaged from 2001 to 10). The bottom panels are zoomed in over the central and eastern Agulhas Bank area for the same decadal mean shown in the middle panels with arrows plotted at the same spatial resolution at AVISO (1/4°). The bold black line is the 200 m isobath.

on the Agulhas Bank. This approach enables the experiments to be run offline, using pre-existing model outputs and has been used extensively to identify advective pathways and variations (e.g., Jacobs et al., 2019; Kelly et al., 2020; Mutia et al., 2021; Wilson et al., 2021).

Experiments are run using multiple point particle releases into the 5-day mean three-dimensional velocity fields of the model (e.g., Popova et al., 2013). Using an analytical method, bilinear interpolation is used to transport the particles through the model grid cells, with particle positions recorded at daily intervals. Although Ariane is sufficiently able to describe advection pathways, it does not account for turbulent mixing and cannot guarantee that particles follow constant density surfaces exactly as it uses 5-day mean velocity fields. However, using multiple releases provides information on the uncertainty associated with different dispersal routes, which is sufficient for this study. It should be noted that this approach seeks to characterise the variability of the large-scale circulation and to identify dispersal pathways that lead to low retention. We suggest that such a pathway identification is a necessary first step in the analysis of the specific behaviours of chokka squid paralarvae which, in addition to passive transport by the ocean currents, has its own (although limited) swimming behavior. The latter is usually investigated using Individual Based Models (IBMs) and is the focus of prior studies (e.g., Martins et al., 2014; Downey-Breedt et al., 2016).

A total of 216 experiments were performed, one for each month from 1995 to 2013. The experiments were initialised at the surface at the beginning of each month and allowed to travel in the model's velocity field for 100 days. Here, we took into account shallow spawning, which is primarily influenced by the surface circulation. Particles were released along the coast from 23.5 to 27°E where bathymetry is < 60 m (Fig. 1), which represents the main chokka squid spawning sites (Sauer et al., 1992). A total of 1470 virtual particles were initialised at the surface per experiment (beginning of each month) where they were uniformly distributed in each model grid cell (25 per grid cell).

To analyse retention, we recorded the proportion of particles that remained on the AB thirty days after release, defined as the 200 m isobath (following Downey-Breedt et al., 2016). Particles that were advected west of 20°E but still remained inside the 200 m isobath (the edge of the AB), as well as those that left the Bank but returned within thirty days, were considered lost. Prior studies assumed that chokka paralarvae were influenced by advection for ~30–45 days after hatching, representing the end of the planktonic phase (e.g., Roberts and Van den Berg, 2002; Vidal et al., 2009; Roberts and Mullon, 2010; Martins et al., 2014; Downey-Breedt et al., 2016). After this, they are reported to hold their position and swim against the prevailing flow (Vidal et al., 2009). As it was difficult to assign an exact time, a period of thirty days was used here (following Roberts and Van den Berg, 2002; Roberts and Mullon, 2010) with the aim of understanding the causes of high or low retention on the AB, as opposed to chokka squid paralarvae behavior.

3. Results

3.1. Seasonal and interannual variability

The monthly proportion of particles, initialised as described in section 2.2, lost from the AB, is shown in Fig. 3. It is highly variable, ranging from 0 to 74% (Table 1). Here, we define high retention (or low loss) events as <10% lost from the AB, which account for 154/216 releases. In contrast, low retention (or high loss) events are defined (subjectively) as >50% lost from the AB and occur for just 4/216 releases, indicating that most of the particles remain on the shelf for the first month. A high proportion of the total particle loss occurs for the East releases (those released east of 25.5°E, Fig. 1) compared with the West releases (Fig. 4). The maximum proportion of particles lost from the AB for the West releases is 43%, whereas >96% are lost during a single event for the East releases (Table 1). The greater risk of loss from the Bank, when released further east, is likely associated with increased interaction with the AC, which flows south-westward along the shelf edge. In contrast, the West releases are more likely to avoid interaction with this fast-flowing current and, instead, are entrained in the slower, westward flow on the Bank. This is further illustrated in Fig. 5, which shows the increased retention, averaged over the entire period, from east to west, for the different release sites. The greater retention of particles released further west could lead to a greater survival rate for chokka that spawn further west.

While the West releases do not exhibit any seasonal variability (Fig. 4c), the East releases experience a clear seasonal cycle (Fig. 4d) in the percentage of particles lost from the AB. Greater retention generally occurs during the austral summer while greater loss occurs during the austral winter from April–August, with more than a quarter of all particles lost from the shelf during June. This is consistent with Martins et al. (2014) and Downey-Breedt et al. (2016) who also found greater losses in winter, which coincides with a weaker AC (Supplementary Fig. 1a). There is no evidence for seasonal changes in the position of the AC in the model at this location (Supplementary Figs. 1b and 2). However, relatively small changes in the position may be masked by the passage of meanders or Natal Pulses, which can cause the AC to deviate

Table 1
Mean, maximum and minimum % of particles lost from the Agulhas Bank and the number of releases exceeding 50% and less than 10% particle loss after 30 days for all releases from 1995 to 2013 (a total of 216), and separated into releases east and west of 25.5°E.

Releases	Mean	Max	Min	>50%	<10%
All	8.42%	74.01%	0%	4	154
East	12.91%	96.27%	0%	11	134
West	1.64%	43.08%	0%	0	205

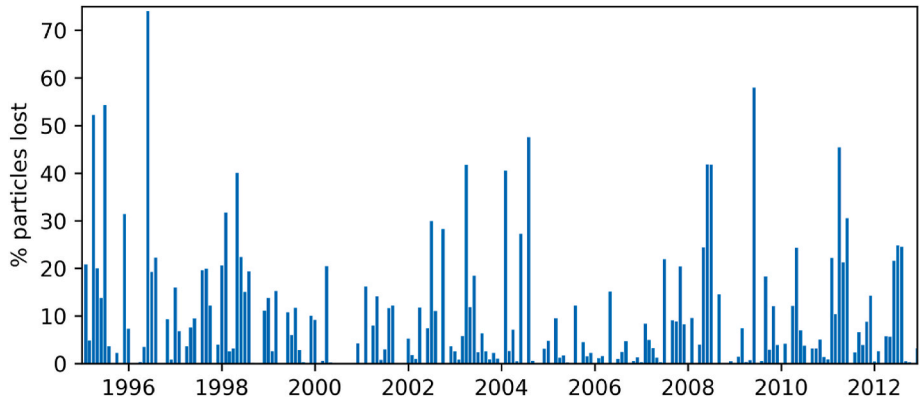

Fig. 3. Percentage of particles lost from the Agulhas Bank (defined by the 200 m isobath) 30 days after each monthly release from 1995 to 2013.

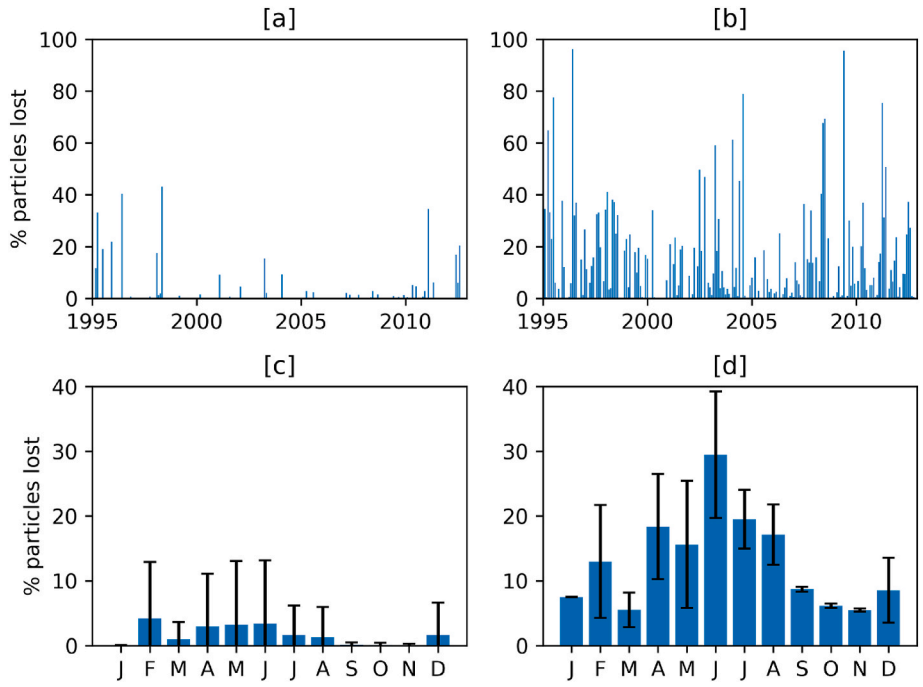

Fig. 4. Percentage of particles lost from the Agulhas Bank (defined by the 200 m isobath) 30 days after release from 1995 to 2015 when released west of [a] and east of 25.5°E [b] and their associated seasonal cycles [c, d]. Bars on [c] and [d] represent the standard deviation.

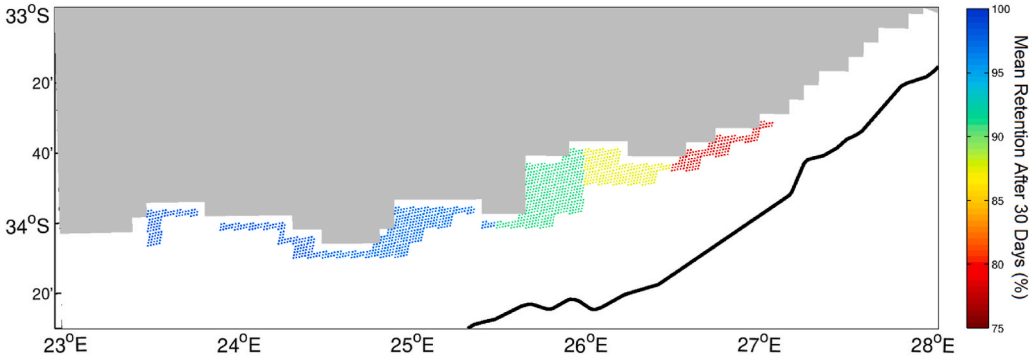

Fig. 5. Mean percentage of particles retained on the Agulhas Bank 30 days after release from 1995 to 2015 for each release location. The black line represents the 200 m isobath.

by up to 200 km from the shelf-edge (Rouault et al., 2010). It is unclear whether the weaker AC is associated with a higher frequency of meanders or Natal Pulses but this is outside the scope of this paper. Despite this, the seasonality experienced by the East releases could be associated with seasonal variations in the speed of the AC.

3.2. High loss events

This section explores the 11 high loss (low retention) events that occurred for the East releases. All events fall into the following three categories that are associated with AC variability modes: i) a meander at the northeast edge of the AB (2 events); ii) when the AC is located further offshore, south of the shelf-edge (6 events), and iii) when a branch of the AC is located further onshore, north of the shelf-edge (3 events). Examples of two events from each category are explored in more detail using trajectory maps, showing the progression of the virtual particles for 60 days and maps of the Eulerian currents (5-day means) to visualise the interaction with the AC. The events selected here are chosen as they are found to best represent the "mode" of AC dynamics for each category. The trajectory maps and associated Eulerian currents for the other events are shown in Supplementary Fig. 3.

Examples of trajectory maps for high loss events are shown in Fig. 6. In June 1996 (Fig. 6a) and August 2004 (Fig. 6b), a meander (Fig. 6c and d) advects a considerable proportion of particles off the shelf, leading to a loss of 96% and 79%, respectively, from the East releases after 30 days. For both events, the timing of the meander causes particles to cross the 200 m isobath within two weeks, with the majority doing so east of 24°E and continuing to flow in the path of the AC towards the southwest. The path taken by the particles is better understood when considering the surface currents for the first 30 days. For example, during June 1996, the meander is seen to progress along the shelf (Fig. 7). When released at the start of June, the particles are seen to slowly flow westward along the shelf (Fig. 6a, red trajectories). This initial slow flow enables the particles to become entrained in a meander that passes the eastern edge of the AB from 13 June (Fig. 7), causing them to flow off the shelf and continue in the AC (Fig. 6a, orange and yellow trajectories). This situation is very similar during August 2004 (Supplementary Fig. 4).

The high loss events in July 1995 (Fig. 8a) and 2008 (Fig. 8b) coincide with periods when the AC is located further offshore (Fig. 8c, d), i.e., south of the 200 m isobath. These events see a 78% and 69% loss

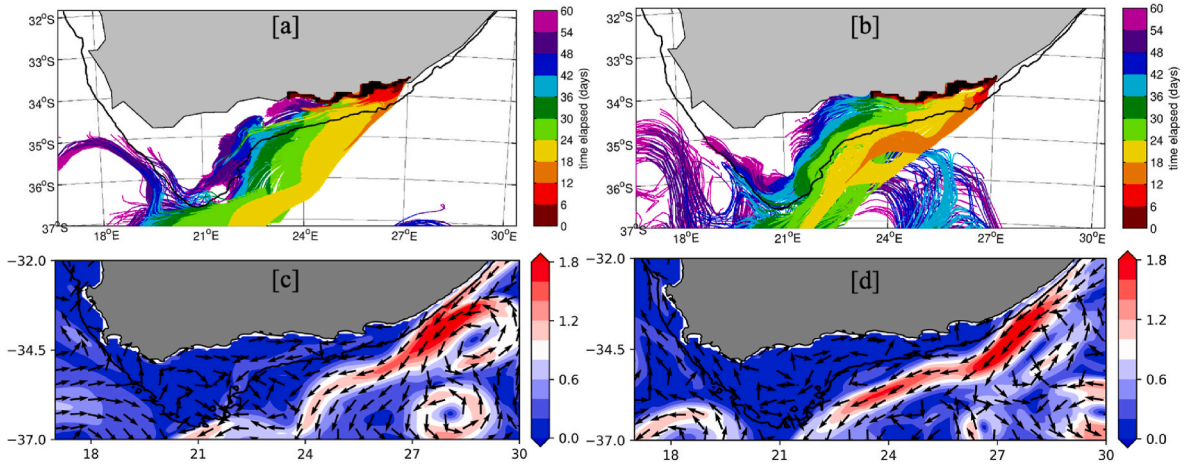

Fig. 6. Trajectory maps during high loss events due to a meander in June 1996 [a] and August 2004 [b]. 5-day mean surface currents m s^{-1} starting from June 13, 1996 [c] and August 12, 2004 [d]. Shaded black on [a, b] indicates the particles' release locations and the black lines is the 200 m isobaths.

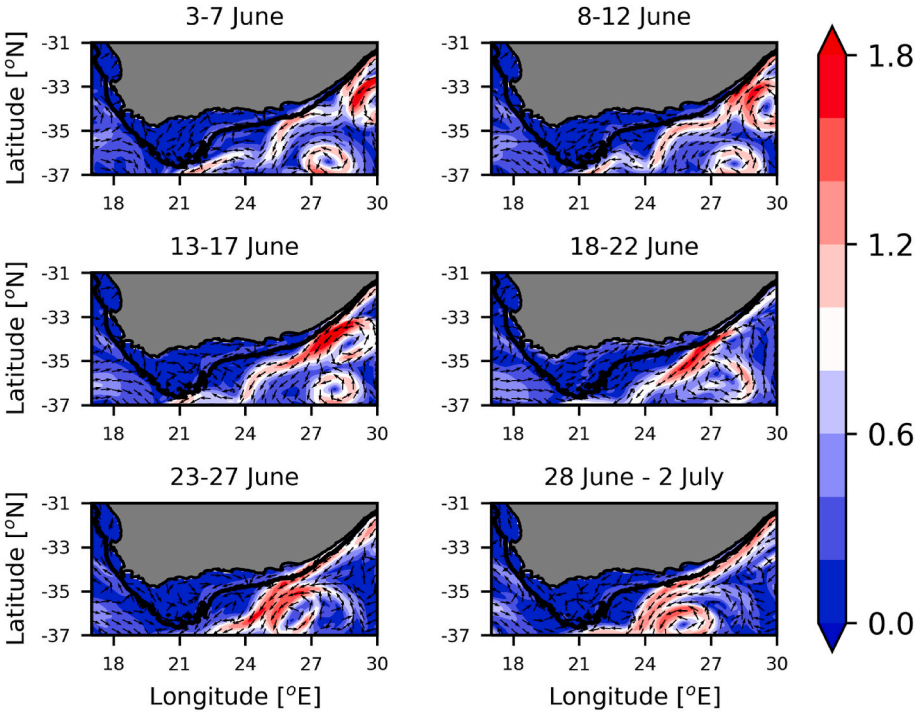

Fig. 7. Modelled 5-day mean surface currents m s^{-1} for June 1996. Black line is the 200 m isobath.

of particles respectively, after 30 days, from the AB for the East releases. Similar to the high loss events associated with meanders, a high proportion of particles are entrained into the AC. As the AC moves offshore, it induces a flow off the Bank, which pulls the particles with it and transports them away from the AB ecosystem. In July 1995 (Fig. 8b), particles follow this pathway and exit the AB from around 18 days after release (yellow trajectories), while the slower flow on the Bank causes westward flow of the particles released further west (Supplementary Fig. 5). The offshore flow occurs much sooner in July 2008 (Fig. 8a), which may be due to a north-eastward counterflow of particles along the eastern AB coast where the likelihood of getting entrained into the main AC is much higher. This earlier entrainment leads to particles leaving the Bank within 1–2 weeks. This initial eastward flow was also found by Roberts and Mullon (2010) and is known to occur sporadically along the coast, inshore of the AC (Boyd et al., 1992; Lamont et al., 2021). Unlike the events associated with meanders, the position of the surface currents remains fairly static for the entire month of July 2008 (Fig. 9). This causes the particles that get entrained in the AC to flow south-westward in a narrow band, as opposed to the broad flow associated with meanders in Fig. 5.

High loss events also occur when a fast-flowing branch of the AC is located on the Bank, i.e., the opposite of that seen in July 1995 and 2008 (Fig. 8). Two such events occur in April 1995 (Fig. 10a) and April 2003 (Fig. 10b), with East release particle losses of 65% and 59%, respectively, after 30 days. However, as opposed to the other high loss events (Figs. 6 and 8) where the majority of particles leave the shelf east of ~24°E, the particles for these two events escape the Bank much further west, from 20 to 22°E, near the Agulhas Bight, as early as 12–18 days after release. Like the other events, there is a pathway where particles flow westwards across the Bank. However, when the flow is faster on the shelf as seen here, they reach 22°E as early as 6 days compared with >30 days for the other high loss events. Figs. 10c and d reveal that both of

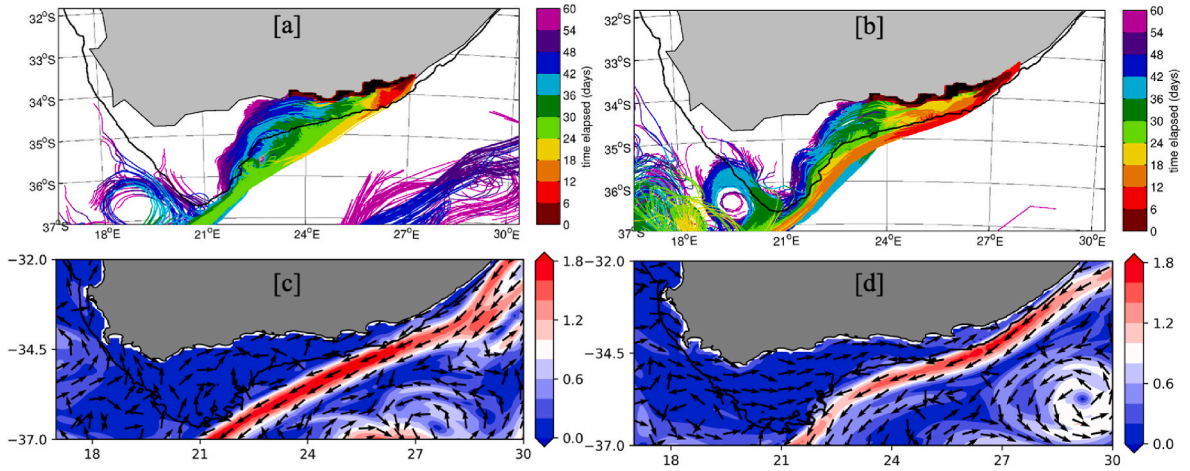

Fig. 8. Trajectory maps during high loss events due to a more offshore Agulhas Current in July 1995 [a] and July 2008 [b]. 5-day mean surface currents m s^{-1} starting from July 4, 1995 [c] and July 8, 2008 [d]. Shaded black indicates the particles' release locations and the black line is the 200 m isobath (see Fig. 1).

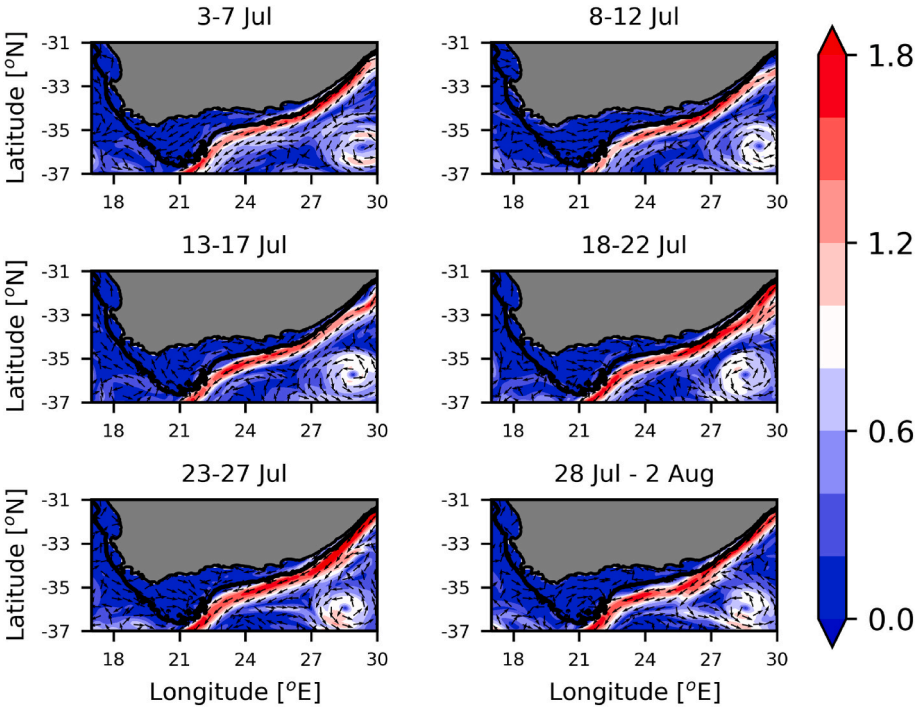

Fig. 9. Modelled 5-day mean surface currents m s^{-1} for July 2008. Black line is the 200 m isobath.

these events are associated with the passage of a Natal Pulse and are larger than the AC meanders seen in Fig. 6. The timing and position of these Natal Pulses, which are very similar, are such that the particles encounter the fast, westward branch of the AC rather than getting entrained offshore in the trailing edge of the Natal Pulse. The progression of the flow in April 2003 (Fig. 11) shows that speeds of >1 ms^{-1} exist on the AB for the first few weeks, enabling the rapid transport of particles to the central AB (Fig. 10b, red and orange trajectories). This rapid westward flow on the leading edge of the Natal Pulse was observed by drifters in 2007 (Hancke et al., this issue). Over the course of the month, this flow on the inshore side of the Natal Pulse moves further onshore as it gradually weakens, keeping the particles on the AB until they are lost further west. The evolution of the currents during this event is remarkably similar during April 1995 (Supplementary Fig. 6).

To summarise, on the AB, high loss events occur when the AC is exhibiting the following variability modes: i) when the AC is located further offshore west of Port Elizabeth, ii) when it is located further onshore from 23 to 26°E, associated with the passage of a Natal Pulse, and iii) when a meander is present in the AC at the northeast edge of the Bank. A meander and an offshore AC will cause most particles to leave the AB east of 24°E so they are lost before reaching the highly productive central AB. This would result in starvation of chokka squid paralarvae and could greatly impact recruitment strength (Roberts, 2005). In contrast, when there is faster flow on the Bank, associated with the leading edge of a Natal Pulse, the particles reach the central AB within a week but continue south-westward and exit the Bank west of 22°E. As the paralarvae remain in the planktonic phase for at least 30 days before being able to swim against the currents, this situation would also likely result in starvation and recruitment failure (Roberts, 2005).

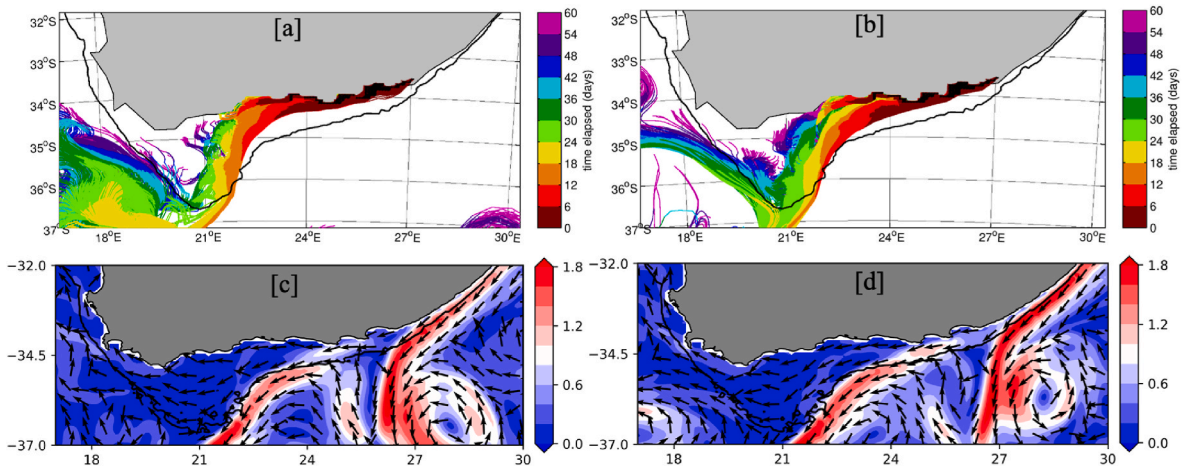

Fig. 10. Trajectory maps during high loss events due to a more onshore Agulhas Current in April 1995 [a] and April 2003 [b]. 5-day mean surface currents m s^{-1} starting from April 5, 1995 [c] and April 5, 2003 [d]. Shaded black indicates the particles' release locations and the black line is the 200 m isobath (see Fig. 1).

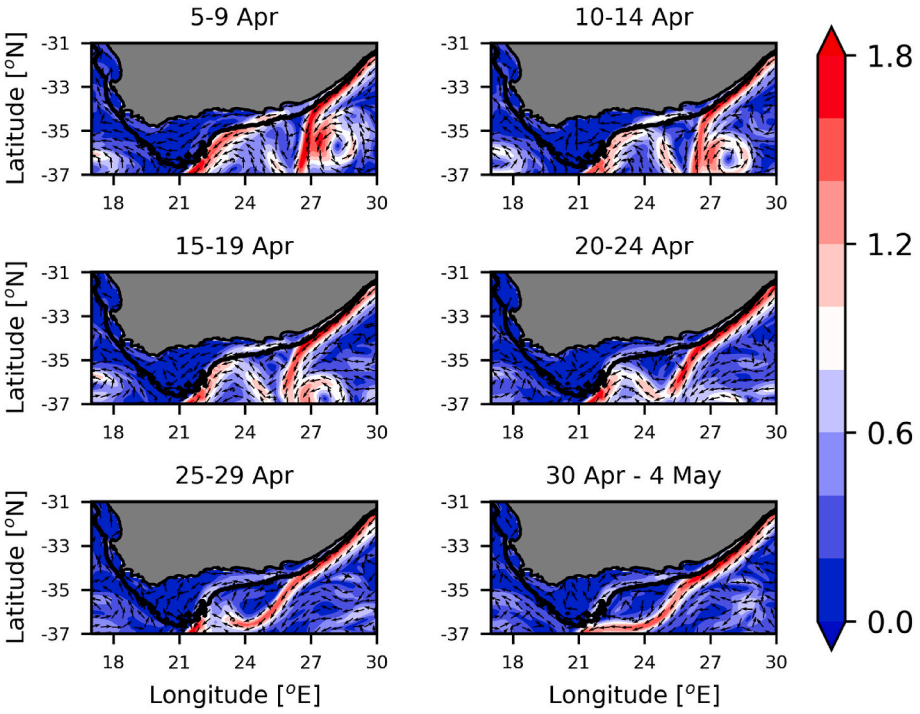

Fig. 11. Modelled 5-day mean surface currents m s^{-1} for April 2003. Black line is the 200 m isobath.

3.3. *High retention events*

Despite the occasional occurrence of high loss events, high retention events are more common, with 154/216 events experiencing >90% retention while nearly a quarter of all events (51/216) experience 100% retention after 30 days. Two such examples from February 2002 (Fig. 12a) and February 2005 (Fig. 12b) show that all particles travel westward across the AB and only exit the Bank after about 2 months, leading to 100% retention after 30 days. Particles initially make a rapid journey (1–2 weeks) to the more productive, central part of the Bank, i.e., the 'Cold Ridge', before continuing west towards the Benguela upwelling system at a much slower pace. This is also seen in surface drifters (Hancke et al. this issue). While the particles from both events encounter slow flow on the AB (Fig. 11c and d), the monthly progression appears quite different for each event. During February 2002 (Supplementary Fig. 7), the AC appears fairly stable, with minimal change in currents on the AB. In contrast, February 2005 is associated with a Natal Pulse (Fig. 13). However, the timing of the Natal Pulse leads to 100% retention of particles after 30 days as opposed to a high loss of particles, as seen in Fig. 10. Note that 4–8th February 2005 (Fig. 13) resembles 15–19th April 2003 (Fig. 11). The particles are still immediately entrained into the westward flow on the AB, i.e., the inshore current associated with the Natal Pulse, but peak speeds are <1 ms^{-1}, meaning the particles spend more time on the AB. This situation is much more beneficial for the chokka squid paralarvae as they need to reach the Cold Ridge quickly in order to feed, and remain for long enough to mature (Roberts, 2005).

4. Discussion and conclusions

The early life history stage for squid generally represents a substantial risk of recruitment failure should the paralarvae not be able to

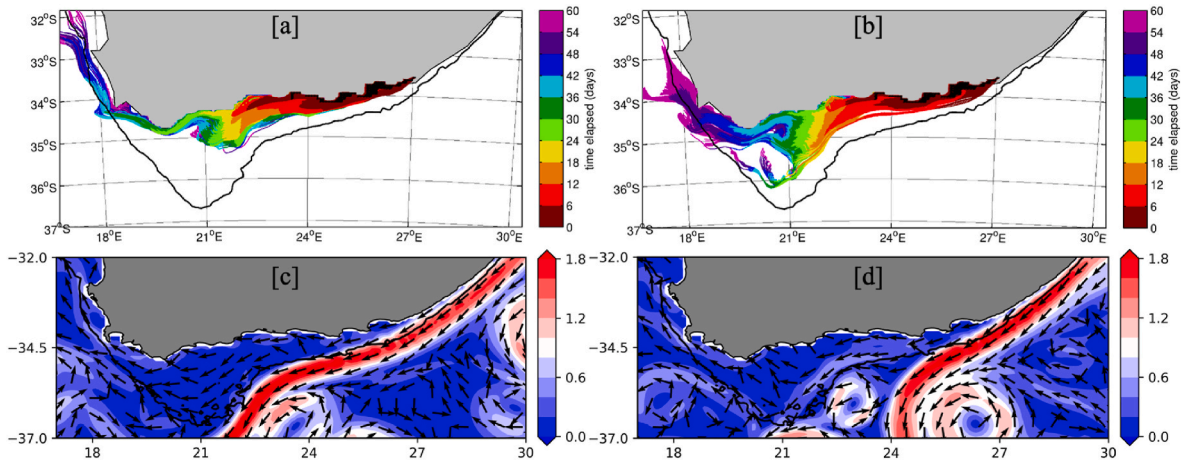

Fig. 12. Trajectory maps during high retention events in February 2002 [a] and February 2005 [b]. 5-day mean surface currents m s^{-1} starting from February 4, 2002 [c] and February 19, 2005 [d]. Shaded black indicates the particles' release locations and the black line is the 200 m isobath (see Fig. 1).

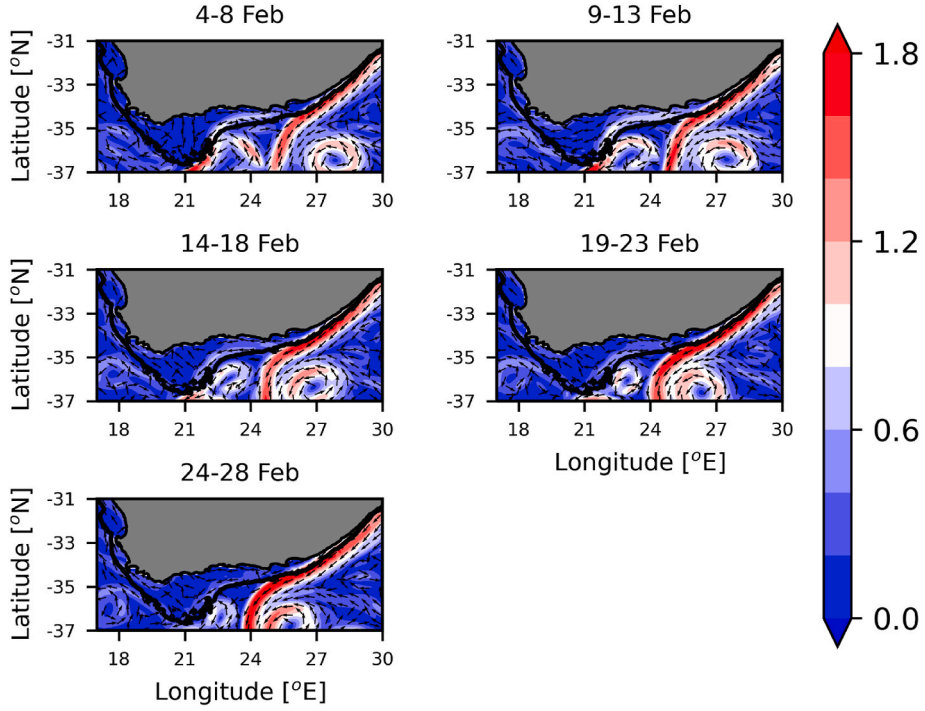

Fig. 13. Modelled 5-day mean surface currents m s^{-1} starting for February 2005. Black line is the 200 m isobath.

find a suitable source of food. For chokka squid, retention is critical to their survival during this early life stage to enable them to utilise the productive AB before being able to swim against the powerful AC (e.g., Vidal et al., 2009). Prior studies, using models of the same spatial resolution as here, have investigated what leads to successful retention on the Bank, i.e., spawning at shallow and sites located further west (Roberts & Mullon; Martins et al., 2014; Downey-Breedt et al., 2016). However, these studies were unable to reliably assess importance of the interannual variability (due to the model using climatological fields) and so could not explore how the frequency of high loss events changes from year to year.

Using a high-resolution global ocean model (NEMO-MEDUSA) and Lagrangian particle tracking, this study assesses the retention properties of the AB relevant to chokka squid life stages. We quantify the proportion of virtual particles, representing chokka squid paralarvae, that are retained on the AB after being released near their main spawning sites. The work builds on that discussed above but with the aim of understanding what causes high loss events and how frequently they occur over an 18-year period.

On monthly timescales, considerable retention variability was found to exist. The most common scenario is high retention (>90%) on the AB after 30 days (154/216 events) but high loss events (up to 74% losses) also occur over the 18-year period. The likelihood of retention was found to have a strong dependency on release location. Particles are much more likely to be lost from the Bank if they are released further east with one particular event leading to a 96% loss of particles for "East releases" (i.e., released east of 25.5°E). In comparison, the highest loss for "West releases" was just 43%. Despite chokka spawning across all release sites (e.g., Lipiński et al., 2016), such a substantial loss from the East releases could still cause a considerable reduction in the survival of chokka paralarvae, which would negatively impact recruitment and potential catch over the AB.

The greater loss of particles released further east is most likely due to their interaction with the AC which is positioned close to the coast in this area. Nonetheless, even the easternmost release sites have a mean retention of 75% over the entire timeseries, indicating high retention in the long-term, with the occasional high loss event leading to more than half the particles (per release) leaving the shelf within 30 days. While the West releases were not found to exhibit a seasonal cycle, the East releases experienced greater losses during the austral winter and reduced losses during the austral summer. This seasonal variability coincides with the seasonality in the strength of the AC with a weaker AC found during the austral winter, which is consistent with prior studies (Lutjeharms, 2006; Krug and Tournadre, 2012; Beal et al., 2015; Beal and Elipot 2016; Hutchinson et al., 2018; Lamont et al., 2021). Near the release sites (34.5°S), no seasonal variability was found in the position of the AC. This may be due to it being at the northeast edge of the AB, which is influenced by the irregular passage of meanders and Natal Pulses (de Ruijter et al., 1999). These features cause AC deviations of 100 s km (e.g., Rouault et al., 2010) and, as they do not exhibit a seasonal cycle, may mask any seasonal cycle that exists in the position of the AC. Apart from the work of Lamont et al. (2021) that finds some evidence of seasonal shift (albeit over a short time period), there is limited evidence for seasonal changes in the position of the AC at various locations. It remains unclear as to why enhanced losses occur alongside a weaker AC so further work is required to understand this seasonal relationship. This has also been identified in other studies (Martins et al., 2014; Downey-Breedt et al., 2016).

On interannual timescales, retention is highly variable with multiple high loss (here defined as >50%) events identified and attributed to AC dynamics. These events are placed into one of the following three modes of AC variability: an AC that is positioned further offshore; an AC that has a fast-flowing branch further onshore, and occurrence of an AC meander that causes offshore flow at the northeast edge of the Bank. Whilst these situations have only led to eleven high loss events over the 18-year period being analysed, it is important to note that it is the timing of these situations, relative to particle release, that leads to changes in retention. For example, only two high loss events were caused by offshore advection in the trailing limb of a meander as it interacted with the virtual particles at the northeast edge of the AB near the release sites. There is evidence that these meanders occurred after the passage of a Natal Pulse (Fig. 6). Whilst there were more than two occurrences of such meanders in the AC over the 18-year period, the timing, relative to particle release, was such that the other meanders did not cause a considerable loss of particles from the AB. Here our focus is not on providing information on the frequency of occurrence of such events but rather on understanding the dynamical processes that could lead to major changes in retention.

Timing is also crucial for understanding what led to the other high loss events. Three such events occurred due to a fast branch of the AC residing slightly further onshore, north of the 200 m isobath, on the inshore side of a Natal Pulse (Fig. 9). It led to the immediate, rapid advection of particles from the release sites across the AB where they were eventually lost west of 22°E within 30 days. The acceleration of south-westward flow on the Bank at the leading edge of a Natal Pulse was also observed using surface drifters during an event in 2007 (Hancke et al., this issue), which supports the model results obtained here.

The remaining high loss events were all associated with an AC that was positioned slightly further offshore, i.e., south of the 200 m isobath. For these events, particles are immediately entrained in the AC at the northeast edge of the AB and are then pulled offshore as the current flows towards the southwest. There is evidence that some of these events are associated with an initial eastward counter-flow along the coast, which increases the likelihood that a larger proportion of particles are entrained in the AC and subsequently advected off the AB. All six of these events occur 1–2 months after the passage of an AC meander or a Natal Pulse.

Natal Pulses evidently exert a strong influence on the retention properties of the AB, with all three types of high loss events associated with different phases of a Natal Pulse. If particles are released when the trailing edge of the Natal Pulse is passing the eastern AB, they are immediately entrained in the onshore flow and advected westwards rapidly before exiting the AB further west. However, if the particles are released into the flow approximately 15 days after this when the onshore flow is weaker and further on the AB, then 100% retention is achieved. Furthermore, in the weeks after this, the AC settles into a more offshore position, again resulting in high losses.

Comparison of the model velocity with that derived from AVISO showed that the model is able to represent the key features of the circulation on the AB and in the AC, including the meanders and Natal Pulses. Surface drifters have also indicated that acceleration of south-westward flow occurs with a Natal Pulse event (Hancke et al., this issue). However, the fast, westward onshore flow occurring during a Natal Pulse may not be an accurate representation of reality, with Rouault and Penven (2011) and Krug et al. (2014) finding evidence for eastward (cyclonic) flow from satellite altimetry AVISO currents. NEMO is a global model, so higher resolution, nested regional models are required to investigate Natal Pulse dynamics. Additionally, AVISO has improved since 2014 (Copernicus, 2021) so more detail may now be included in the gridded altimetry product. Increased spatial and temporal resolution would also likely lead to more accurate results due to the dynamic and sub-mesoscale nature of this shelf region and should be the focus of future work. Additionally, now that these pathways have been identified, understanding the local and remote forcing that may initiate these changes in the AC would also be an appropriate avenue for future work.

Despite the occasional high loss event, the most common situation is high retention (>90%). This is the best scenario for chokka squid paralarvae at this stage of their life cycle as it transports them to the productive feeding grounds on the central AB, i.e., the Cold Ridge, and retains them on the Bank for at least 30 days until they have matured enough to be able to swim against the strong currents (Vidal et al., 2009). This is more likely to lead to greater survival and have positive impacts on recruitment, leading to a potentially greater catch. The question remains as to whether a singular or a succession of high loss events occurred during peak spawning and led to the low catch in 2013. There is evidence for a Natal Pulse in the gridded altimetry AVISO currents in April 2012 and May 2013 (not shown) with multiple meanders also evident in 2012 and 2013. These events may have increased the loss of paralarvae from the AB ecosystem, leading to recruitment failure and decreasing the catch for 2013 as, following Bruggeman et al. (this issue), reduced catches would occur approximately 9 months later. This approach is insufficient to evidence the cause of the low catch so an IBM model is required, which accounts for advection, productivity and the life history of the chokka squid. A substantial advance can be made via a systematic analysis of AC topology using remote sensing to establish whether there was an increased frequency of meanders and Natal Pulses in the lead up to 2013 compared with other years.

As the ocean components of the current Earth System Models used for IPCC-class future projections are still of the order of 1°, it is unclear how the AC may respond to future climate change, although there is evidence for increased eddy activity leading to an overall broadening of the current since the 1990s (Beal and Elipot, 2016). Future projections using ocean-only models indicate that the AC may shift onshore over the coming century (Asdar et al., this issue), which may increase the occurrence of high loss events and, consequently, lead to poor recruitment of chokka squid. However, the spatial resolution of the ocean future projection (1/4°) used in the Asdar et al. (this issue) study is not yet high enough to simulate Natal Pulses, and an even further increase of resolution is required.

To summarise, this study finds that greater losses of virtual particles occur from the release sites that are located further east due to increased interaction with the AC. However, even the easternmost releases

experience an average retention of 75% within 30 days. At seasonal scales, greater losses are found to coincide with a weaker AC in the austral winter. Despite high retention (>90%) being the most common occurrence, a number of high loss (>50%) events are also apparent on interannual timescales, which could cause a considerable reduction in the survival of chokka squid paralarvae if it occurs at the time of peak spawning. Consequently, this could cause recruitment failure and a dent in catch. All high loss events were found to be associated with a passage of a Natal Pulse, but the timing of such events relative to the spawning is crucial as the same dynamical feature can both increase and reduce the retention of larvae, depending on the location of the spawning. Further work needs to be done to ascertain whether a higher frequency of such events has an influence on the chokka squid catch, with the potential for an early warning system to be put in place.

Author contribution statement

Z.J. developed the original idea, produced description of the results and most of the key figures. E.P. contributed to the design of the Lagrangian particle tracking experiments, which were conducted by S.K. who also produced the trajectory figures. E.P., F.J., M.S., M.R. and W.S. contributed to the interpretation and discussion of the results. E.P. and M.R. contributed to the development of the idea. L.H, M.R. and W.S. contributed to the development of the introduction and discussion. All authors contributed to the improvement of the paper, made edits and reviewed the final manuscript. E.P. coordinated the study.

Declaration of competing interest

The authors declare that they have no known competing financial interests or personal relationships that could have appeared to influence the work reported in this paper.

Acknowledgements

This publication was produced with the financial support of the Global Challenges Research Fund (GCRF) in the framework of the SOLSTICE-WIO project, NE/P021050/1. This work is also part of the UK-SA Bilateral Chair in Ocean Science and Marine Food Security funded by the British Council Newton Fund grant SARCI 1503261 16102/NRF98399. We acknowledge the NEMO consortium for the modelling framework used in this study. The model run was performed using the ARCHER UK National Supercomputing with outputs stored at the Centre for Environmental Data Analysis JASMIN servers and can be provided upon request. The Ariane software was developed by B. Blanke and N. Grima.

Appendix A. Supplementary data

Supplementary data to this article can be found online at https://doi.org/10.1016/j.dsr2.2022.105151.

References

Asdar, M., Jacobs, Z., Popova, E., Noyon, M., Sauer, W.H.H., Roberts, M. This issue. Projected climate change impacts on the ecosystems of the Agulhas Bank, South Africa. Deep-Sea Res.II.

Augustyn, C.J., Lipiński, M.R., Sauer, W.H.H., 1992. Can the Loligo squid fishery be managed effectively? A synthesis of research on Loligo vulgaris reynaudii. S. Afr. J. Mar. Sci. 12 (1), 903–918. https://doi.org/10.2989/02577619209504751.

Augustyn, C.J., Lipinski, M.R., Roberts, M.J., Mitchell-Innes, B.A., Sauer, W., 1994. Chokka squid on the Agulhas Bank: life history and ecology. South Afr. J. Sci. 90 (3). https://hdl.handle.net/10520/AJA00382353_4623.

Bakun, A., 1998. Ocean triads and radical interdecadal variation: bane and boon to scientific fisheries management. In: Reinventing Fisheries Management. Springer, Dordrecht, pp. 331–358. https://doi.org/10.1007/978-94-011-4433-9_25.

Beal, L.M., Elipot, S., Houk, A., Leber, G.M., 2015. Capturing the transport variability of a western boundary jet: results from the Agulhas current time-series experiment (ACT). J. Phys. Oceanogr. 45 (5), 1302–1324. https://doi.org/10.1175/JPO-D-14-0119.1.

Beal, L.M., Elipot, S., 2016. Broadening not strengthening of the Agulhas Current since the early 1990s. Nature 540 (7634), 570–573. https://doi.org/10.1038/nature19853.

Bigelow, K.A., 1992. Age and growth in paralarvae of the mesopelagic squid Abralia trigonura based on daily growth increments in statoliths. Mar. Ecol. Progr. Ser. Oldendorf 82 (1), 31–40. https://doi.org/10.1016/B978-0-12-800287-2.00004-4.

Blanke, B., Delecluse, P., 1993. Variability of the tropical Atlantic Ocean simulated by a general circulation model with two different mixed-layer physics. J. Phys. Oceanogr. 23 (7), 1363–1388.

Blanke, B., Raynaud, S., 1997. Kinemati cs of the Pacific equatorial undercurrent: an Eulerian and Lagrangian approach from GCM results. J. Phys. Oceanogr. 27 (6), 1038–1053. https://doi.org/10.1175/1520-0485(1997)027<1038:KOTPEU>2.0.CO;2.

Boyd, A.J., Shillington, F.A., 1994. Physical forcing and circulation patterns on the Agulhas Bank. South Afr. J. Sci. 90 (3), 143–154. https://hdl.handle.net/10520/AJA00382353_4624.

Boyd, A.J., Taunton-Clark, J., Oberholster, G.P.J., 1992. Spatial features of the near-surface and midwater circulation patterns off western and southern South Africa and their role in the life histories of various commercially fished species. S. Afr. J. Mar. Sci. 12 (1), 189–206. https://doi.org/10.2989/02577619209504702.

Brodeau, L., Barnier, B., Treguier, A.M., Penduff, T., Gulev, S., 2010. An ERA40-based atmospheric forcing for global ocean circulation models. Ocean Model. 31 (3–4), 88–104. https://doi.org/10.1016/j.ocemod.2009.10.005.

Bruggeman, J., Jacobs, Z., Popova, E., Sauer, W.H.H., Gornall, J.M., Brewin, R.J.W., Roberts, M.J. This issue. The paralarval stage as key to predicting squid catch: hints from a process-based model. Deep-Sea Res. II.

Cochrane, K.L., Oliver, B., Sauer, W., 2014. An assessment of the current status of the chokka squid fishery in South Africa and an evaluation of alternative allocation strategies. Mar. Pol. 43, 149–163. https://doi.org/10.1016/j.marpol.2013.05.006.

Copernicus, 2021. https://catalogue.marine.copernicus.eu/documents/QUID/CMEMS-SL-QUID-008-056-058.pdf.

Cravatte, S., Madec, G., Izumo, T., Menkes, C., Bozec, A., 2007. Progress in the 3-D circulation of the eastern equatorial Pacific in a climate ocean model. Ocean Model. 17 (1), 28–48. https://doi.org/10.1016/j.ocemod.2006.11.003.

de Ruijter, W.P., Van Leeuwen, P.J., Lutjeharms, J.R., 1999. Generation and evolution of natal Pulses: solitary meanders in the Agulhas current. J. Phys. Oceanogr. 29 (12), 3043–3055. https://doi.org/10.1175/1520-0485(1999)029<3043:GAEONP>2.0.CO;2.

Downey-Breedt, N.J., Roberts, M.J., Sauer, W.H., Chang, N., 2016. Modelling transport of inshore and deep-spawned chokka squid (Loligo reynaudi) paralarvae off South Africa: the potential contribution of deep spawning to recruitment. Fish. Oceanogr. 25 (1), 28–43. https://doi.org/10.1111/fog.12132.

Dussin, R., Barnier, B., Brodeau, L., Molines, J.M., 2016. The making of DRAKKAR forcing set DFS5. DRAKKAR/MyOcean Rep. 01-04- 16. Retrieved from. https://www.drakkar-ocean.eu/publications/reports/report_DFS5v3_April2016.pdf.

Goschen, W.S., Schumann, E.H., 1988. ocean current and temperature structures in Algoa Bay and beyond in November 1986. S. Afr. J. Mar. Sci. 7 (1), 101–116. https://doi.org/10.2989/025776188784379198.

Gründlingh, M.L., 1979. Observation of a large meander in the Agulhas current. J. Geophys. Res.: Oceans 84 (C7), 3776–3778. https://doi.org/10.1029/JC084iC07p03776.

Hancke et al.. This issue. Insights of circulation from surface drifters. Deep Sea Res. Part II Top. Stud. Oceanogr..

Huggett, J.A., Richardson, A.J., 2000. A review of the biology and ecology of Calanus agulhensis off South Africa. ICES (Int. Counc. Explor. Sea) J. Mar. Sci. 57 (6), 1834–1849. https://doi.org/10.1006/jmsc.2000.0977.

Hutchings, L., Van der Lingen, C.D., Shannon, L.J., Crawford, R.J.M., Verheye, H.M.S., Bartholomae, C.H., et al., 2009. The Benguela Current: an ecosystem of four components. Prog. Oceanogr. 83 (1–4), 15–32. http://hdl.handle.net/10204/6572.

Hutchinson, K., Beal, L.M., Penven, P., Ansorge, I., Hermes, J., 2018. Seasonal phasing of Agulhas current transport tied to a Baroclinic adjustment of near-field winds. J. Geophys. Res.: Oceans 123 (10), 7067–7083. https://doi.org/10.1029/2018JC014319.

Jackson, J.M., Rainville, L., Roberts, M.J., McQuaid, C.D., Lutjeharms, J.R., 2012. Mesoscale bio-physical interactions between the Agulhas current and the Agulhas Bank, South Africa. Continent. Shelf Res. 49, 10–24. https://doi.org/10.1016/j.csr.2012.09.005.

Jacobs, Z.L., Grist, J.P., Marsh, R., Josey, S.A., 2019. A subannual subsurface pathway from the Gulf Stream to the Subpolar Gyre and its role in warming and salinification in the 1990s. Geophys. Res. Lett. 46 (13), 7518–7526. https://doi.org/10.1029/2019GL083021.

Jacobs, Z.L., Jebri, F., Raitsos, D.E., Popova, E., Srokosz, M., Painter, S.C., et al., 2020. Shelf-break upwelling and productivity over the North Kenya Banks: the importance of large-scale ocean dynamics. J. Geophys. Res.: Oceans 125 (1), e2019JC015519.

Jacobs, Z., Roberts, M., Jebri, J., Srokosz, M., Kelly, S., Sauer, W.H.H., Bruggeman, J., Popova, E. This issue. Drivers of productivity on the Agulhas Bank and the importance for marine ecosystems. Deep-Sea Res. II..

Kelly, S.J., Popova, E., Aksenov, Y., Marsh, R., Yool, A., 2020. They came from the Pacific: how changing Arctic currents could contribute to an ecological regime shift in the Atlantic Ocean. Earth's Future 8 (4), e2019EF001394. https://doi.org/10.1029/2019EF001394.

Krug, M., Tournadre, J., 2012. Satellite observations of an annual cycle in the Agulhas Current. Geophys. Res. Lett. 39 (15) https://doi.org/10.1029/2012GL052335.

Krug, M., Tournadre, J., Dufois, F., 2014. Interactions between the Agulhas current and the eastern margin of the Agulhas Bank. Continent. Shelf Res. 81, 67–79. https://doi.org/10.1016/j.csr.2014.02.020.

Lamont, T., Louw, G.S., Russo, C.S., van den Berg, M.A., 2021. Observations of northeastward flow on a narrow shelf dominated by the Agulhas Current. Estuar. Coast Shelf Sci. 251, 107197 https://doi.org/10.1016/j.ecss.2021.107197.

Leber, G.M., Beal, L.M., 2014. Evidence that Agulhas Current transport is maintained during a meander. J. Geophys. Res.: Oceans 119 (6), 3806–3817. https://doi.org/10.1002/2014JC009802.

Leber, G.M., Beal, L.M., Elipot, S., 2017. Wind and current forcing combine to drive strong upwelling in the Agulhas Current. J. Phys. Oceanogr. 47 (1), 123–134. https://doi.org/10.1175/JPO-D-16-0079.1.

Levitus, S., Conkright, M., Boyer, T.P., O'Brian, T., Antonov, J., Stephens, C., et al., 1998. World Ocean Database 1998. Technical Report NESDIS 18, NOAA Atlas.

Lipiński, M.R., Van der Vyver, J.S.F., Shaw, P., Sauer, W.H.H., 2016. Life cycle of chokka-squid Loligo reynaudii in South African waters. Afr. J. Mar. Sci. 38 (4), 589–593. https://doi.org/10.2989/1814232X.2016.1230074.

Lutjeharms, J.R.E., Roberts, H.R., 1988. The Natal pulse: an extreme transient on the Agulhas Current. J. Geophys. Res.: Oceans 93 (C1), 631–645. https://doi.org/10.1029/JC093iC01p00631.

Lutjeharms, J.R.E., Catzel, R., Valentine, H.R., 1989. Eddies and other boundary phenomena of the Agulhas Current. Continent. Shelf Res. 9 (7), 597–616. https://doi.org/10.1016/0278-4343(89)90032-0.

Lutjeharms, J.R., 2006. The Agulhas Current, vol. 329. Springer, Berlin.

Madec, G., 2015. NEMO Ocean Engine.

Madec, G., Imbard, M., 1996. A global ocean mesh to overcome the North Pole singularity. Clim. Dynam. 12 (6), 381–388.

Malan, N., Durgadoo, J.V., Biastoch, A., Reason, C., Hermes, J., 2019. Multidecadal wind variability drives temperature shifts on the Agulhas Bank. J. Geophys. Res.: Oceans 124 (5), 3021–3035. https://doi.org/10.1029/2018JC014614.

Martins, R.S., Roberts, M.J., Lett, C., Chang, N., Moloney, C.L., Camargo, M.G., Vidal, E. A., 2014. Modelling transport of chokka squid (Loligo reynaudii) paralarvae off South Africa: reviewing, testing and extending the 'Westward Transport Hypothesis. Fish. Oceanogr. 23 (2), 116–131. https://doi.org/10.1111/fog.12046.

Marzocchi, A., Hirschi, J.J.M., Holliday, N.P., Cunningham, S.A., Blaker, A.T., Coward, A.C., 2015. The North Atlantic subpolar circulation in an eddy-resolving global ocean model. J. Mar. Syst. 142, 126–143. https://doi.org/10.1016/j.jmarsys.2014.10.007.

Moat, B.I., Josey, S.A., Sinha, B., Blaker, A.T., Smeed, D.A., McCarthy, G., Johns, W.E., Hirschi, J.M., Frajka-Williams, E., Rayner, D., Duchez, A., 2016. Major variations in subtropical North Atlantic heat transport at short (5 day) timescales and their causes. J. Geophys. Res.: Oceans 121, 3237–3249. https://doi.org/10.1002/2016JC011660.

Mutia, D., Carpenter, S., Jacobs, Z., Jebri, F., Kamau, J., Kelly, S.J., et al., 2021. Productivity driven by Tana river discharge is spatially limited in Kenyan coastal waters. Ocean Coast Manag. 211, 105713 https://doi.org/10.1016/j.ocecoaman.2021.105713.

Penven, P., Cambon, G., Tan, T.A., Marchesiello, P., & Debreu, L. (2010). ROMS AGRIF/ROMSTOOLS.

Popova, E.E., Yool, A., Aksenov, Y., Coward, A.C., 2013. Role of advection in Arctic Ocean lower trophic dynamics: a modeling perspective. J. Geophys. Res.: Oceans 118 (3), 1571–1586. https://doi.org/10.1002/jgrc.20126.

Roberts, M.J., Van den Berg, M., 2002. Recruitment variability of chokka squid (Loligo vulgaris reynaudii)—role of currents on the Agulhas Bank (South Africa) in paralarvae distribution and food abundance. Bull. Mar. Sci. 71 (2), 691–710.

Roberts, M.J., 2005. Chokka squid (Loligo vulgaris reynaudii) abundance linked to changes in South Africa's Agulhas Bank ecosystem during spawning and the early life cycle. ICES (Int. Counc. Explor. Sea) J. Mar. Sci. 62 (1), 33–55. https://doi.org/10.1016/j.icesjms.2004.10.002.

Roberts, M.J., Mullon, C., 2010. First Lagrangian ROMS–IBM simulations indicate large losses of chokka squid Loligo reynaudii paralarvae from South Africa's Agulhas Bank. Afr. J. Mar. Sci. 32 (1), 71–84. https://doi.org/10.2989/18142321003714518.

Rouault, M.J., Penven, P., 2011. New perspectives on Natal Pulses from satellite observations. J. Geophys. Res.: Oceans 116 (C7). https://doi.org/10.1029/2010JC006866.

Rouault, M.J., Mouche, A., Collard, F., Johannessen, J.A., Chapron, B., 2010. Mapping the Agulhas Current from Space: an Assessment of ASAR Surface Current Velocities.

Russo, C.S., Lamont, T., Krug, M., 2021. Spatial and temporal variability of the Agulhas Retroflection: observations from a new objective detection method. Rem. Sens. Environ. 253, 112239 https://doi.org/10.1016/j.rse.2020.112239.

Sauer, W.H.H., Smale, M.J., Lipinski, M.R., 1992. The location of spawning grounds, spawning and schooling behaviour of the squid Loligo vulgaris reynaudii (Cephalopoda: Myopsida) off the Eastern Cape Coast, South Africa. Mar. Biol. 114 (1), 97–107.

Sauer, W.H., Roberts, M.J., Lipinski, M.R., Smale, M.J., Hanlon, R.T., Webber, D.M., O'Dor, R.K., 1997. Choreography of the squid's" nuptial dance. Biol. Bull. 192 (2), 203–207.

Swart, V.P., Largier, J.L., 1987. Thermal structure of Agulhas Bank water. S. Afr. J. Mar. Sci. 5 (1), 243–252. https://doi.org/10.2989/025776187784522153.

Timmermann, R., Goosse, H., Madec, G., Fichefet, T., Ethe, C., Duliere, V., 2005. On the representation of high latitude processes in the ORCA-LIM global coupled sea ice–ocean model. Ocean Model. 8 (1–2), 175–201. https://doi.org/10.1016/j.ocemod.2003.12.009.

U.S. Department of Commerce, 2006. National geophysical data center: 2-minute gridded global relief data (ETOPO2v2). In: Tech. Rep, vol. 2006. National Oceanic and Atmospheric Administration.

Vidal, E.A.G., Zeidberg, L.D., Buskey, E.J., 2009. Swimming behavior in fed and starved squid paralarvae. CIAC 2009 Symp. Abst Book, Vigo.

Wilson, R.J., Sailley, S.F., Jacobs, Z.L., Kamau, J., Mgeleka, S., Okemwa, G.M., et al., 2021. Large projected reductions in marine fish biomass for Kenya and Tanzania in the absence of climate mitigation. Ocean Coast Manag. 215, 105921 https://doi.org/10.1016/j.ocecoaman.2021.105921.

Yang, W.T., 1983. Growth, behavior and sexual maturation of the market squid, Loligo opalescens, cultured through the life cycle. Fish. Bull. 84, 771–798.